Model investigation of transverse momentum cumulants of different orders in nuclear-nuclear collisions

Zviagina A.P., Andronov E.V.

September 21, 2023

Outline of the report

- Motivation
- Models EPOS, SMASH, PHSD, UrQMD: basic principles
- Quantities used for analysis
- Results for strongly intensive variables: p+p
- Results for cumulants: p+p
- Results for various samples by rapidity intervals: p+p.
- Comparison of two method: p+p
- Results for strongly intensive variables: Bi+Bi
- Results for cumulants: Bi+Bi
- Conclusion

Motivation

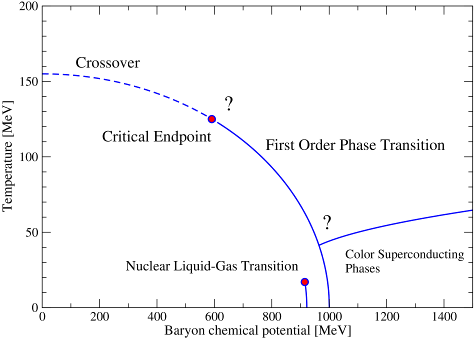

Figure 1: QCD phase transition diagram.

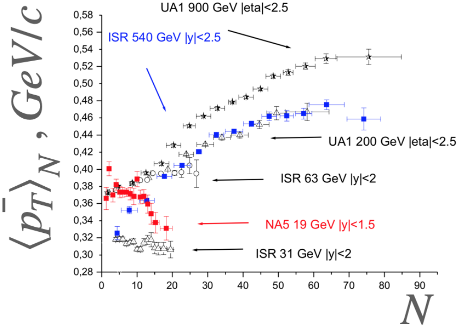

Figure 2: Compilation of experimental results for $p_T - N$ correlations for various experiments and energies.

- transition from negative to positive correlations: multipomeric model [N. Armestoet al., Phys. of Atom. Nucl., 71. 2087-2095 (2008)]
- restrictions for models (PYTHIA, Herwig++ and etc.)

Models

- EPOS (*Energy-conserving quantum mechanical multiple scattering approach, based on Partons (parton ladders), Off-shell remnants, and Splitting of parton ladders*). This model [K. Werner*et al.*, Phys.Rev. C**74**, 044902 (2006)]takes into account the multiple scattering approach based on partons and pomerons (parton ladders). It is based on a string model.

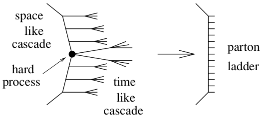

Figure 3: Closed parton ladder.

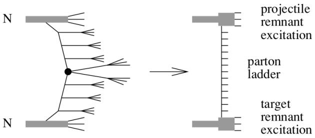

Figure 4: Open parton ladder.

- SMASH (*Simulating Many Accelerated Strongly-interacting Hadrons*) is a relativistic hadron transport approach [J. Weil*et al.*, arXiv:1606.06642 [nucl-th] (2017)]. Includes all known hadrons with mass up to ~ 2 GeV as degrees of freedom.
- PHSD (*Parton-Hadron-String Dynamics*)[E. Bratkovskaya *et al.*, arXiv:1908.00451 [nucl-th] (2019)] presents a microscopic out-of-shell transport approach to describe strongly interacting hadronic and partonic matter in and out of equilibrium.
- UrQMD (*Ultra-relativistic Quantum Molecular Dynamics*)[M. Bleicher et al., arXiv:hep-ph/9909407 [hep-ph] (1999).] is a microscopic model used to simulate (ultra)relativistic heavy ion collisions in the energy range from Bevalac and SIS to AGS, SPS and RHIC.

Definitions and observables: strongly intensive quantities

Types of quantities: strongly intensive, intensive and extensive.
Strongly intensive quantities do not depend either on the volume of the system or on fluctuations in the volume of the system.

$$\omega[N] = \frac{\langle N^2\rangle - \langle N\rangle^2}{\langle N\rangle} - \text{ extensive quantitie} \tag{1}$$

$$\Delta[p_t, N] = \frac{1}{\langle N\rangle\omega\,[p_t]}\left[\langle N\rangle\omega\,[P_t] - \langle P_t\rangle\omega\,[N]\right] - \text{ strongly intensive quantitie} \tag{2}$$

$$\Sigma[p_t, N] = \frac{1}{\langle N\rangle\omega\,[p_t]}\left[\langle N\rangle\omega\,[P_t] + \langle P_t\rangle\omega\,[N] - 2\left(\langle P_T N\rangle - \langle P_T\rangle\langle N\rangle\right)\right] - \text{ strongly intensive quantitie} \tag{3}$$

[M. Gorenstein, M. Gazdzicki, Phys. Rev. C 84, 014904 (2011)]
where $P_T = \sum_{i=1}^{N} p_{T_i}$, and $\omega[p_T]$ is the scaled variance of the inclusive p_T spectrum. $\Delta[p_T, N] = \Sigma[p_T, N] = 1$ - value for the independent particle production model, $\Delta[p_T, N] = \Sigma[p_T, N] = 0$ - in the absence of fluctuations.
Also, another strongly intensive quantity [M. Cody, S. Gavin, B. Koch et al., Phys. Rev. C 107, 014909 (2023)]:

$$\langle N\rangle D[p_t, N] = \frac{1}{\langle N\rangle}\left[\left(\langle P_T N\rangle - \langle P_T\rangle\langle N\rangle\right) - \langle P_t\rangle\omega\,[N]\right] \tag{4}$$

Common define of cumulant

The average of $Q(A_1, ..., A_n)$ over many collision events is a weighted integral of $f(p_1, ..., p_n)$:

$$\langle Q(A_1, ..., A_n)\rangle = \int_p q_1(p_1)...q_n(p_n)f(p_1, ..., p_n) \tag{5}$$

We refer to such averages as *moments*. The cumulant decomposition applies to moments after multiplying equations (2) and (3) by $q_i(p_i)$ and integrating over p_i. The cumulant of order 2 is thus given by the inversion formula

$$\langle Q(A_1, A_2)\rangle_c \equiv \langle Q(A_1, A_2)\rangle - \langle Q(A_1)\rangle\langle Q(A_2)\rangle \tag{6}$$

$$\langle Q_1 Q_2\rangle_c \equiv \langle Q_1 Q_2\rangle - \langle Q_1\rangle\langle Q_2\rangle \tag{7}$$

$$\langle Q_1 Q_2 Q_3\rangle_c \equiv \langle Q_1 Q_2 Q_3\rangle - \tag{8}$$

$$\langle Q_1 Q_2\rangle\langle Q_3\rangle - \tag{9}$$

$$\langle Q_2 Q_3\rangle\langle Q_1\rangle - \tag{10}$$

$$\langle Q_1 Q_3\rangle\langle Q_2\rangle + \tag{11}$$

$$2\langle Q_1\rangle\langle Q_2\rangle\langle Q_3\rangle \tag{12}$$

Note that the cumulant is unchanged if one shifts Q_i by a constant value. This property of translational invariance, which is true to all orders, explains why cumulants are remarkably stable with respect to detector imperfections.

[Ph. Di Francesco *et al.*, Phys. Rev. C 95, 044911 (2017)]

Standart method

The n-particle correlator for p_T in one event is defined as:

$$C_n = \frac{\sum_{i_1 \neq \ldots \neq i_n} \omega_{i_1} \ldots \omega_{i_n} (p_{T,i_1} - \langle\langle p_T \rangle\rangle) \ldots (p_{T,i_n} - \langle\langle p_T \rangle\rangle)}{\sum_{i_1 \neq \ldots \neq i_n} \omega_{i_1} \ldots \omega_{i_n}} \tag{13}$$

$$\kappa_2 = \frac{\langle C_2 \rangle}{\langle\langle p_T \rangle\rangle^2}, \; \kappa_3 = \frac{\langle C_3 \rangle}{\langle\langle p_T \rangle\rangle^3}, \tag{14}$$

where ω_i is the weight for particle i. Cumulants are calculated by averaging c_n over a given ensemble of events.

$$p_{mk} = \sum_i \omega_i^k p_i^m / \sum_i \omega_i^k, \tau_k = \frac{\omega_i^{k+1}}{\left(\sum_i \omega_i\right)^{k+1}} \tag{15}$$

denoting $p \equiv p_T$:

$$\overline{p}_{1k} \equiv p_{1k} - \langle\langle p_T \rangle\rangle \tag{16}$$

$$\overline{p}_{2k} \equiv 2p_{1k} \langle\langle p_T \rangle\rangle + \langle\langle p_T \rangle\rangle^2 \tag{17}$$

$$\overline{p}_{3k} \equiv p_{3k} - 3p_{2k} \langle\langle p_T \rangle\rangle + 3p_{1k} \langle\langle p_T \rangle\rangle^2 - \langle\langle p_T \rangle\rangle^3 \tag{18}$$

$$\overline{p}_{4k} \equiv p_{4k} - 4p_{3k} \langle\langle p_T \rangle\rangle + 6p_{2k} \langle\langle p_T \rangle\rangle^2 - 4p_{1k} \langle\langle p_T \rangle\rangle^3 + \langle\langle p_T \rangle\rangle^4 \tag{19}$$

[Bhatta S. *et. al.* Phys. Rev. C 105, 024904]

Standart method

Note that $\langle\langle p_T \rangle\rangle = \langle p_{11} \rangle$ is the mean value of p_T averaged over ensemble of events.

$$C_2 = \frac{\overline{p}_{11}^2 - \overline{p}_{22}}{1 - \tau_1} \tag{20}$$

$$C_3 = \frac{\overline{p}_{11}^3 - 3\overline{p}_{22}\overline{p}_{11} + 2\overline{p}_{33}}{1 - 3\tau_1 + 2\tau_2} \tag{21}$$

$$C_4 = \frac{\overline{p}_{11}^4 - 6\overline{p}_{22}\overline{p}_{11}^2 + 3\overline{p}_{22}^2 + 8\overline{p}_{33}\overline{p}_{11} - 6\overline{p}_{44}}{1 - 6\tau_1 + 3\tau_1^2 + 8\tau_2 - 6\tau_3} \tag{22}$$

$$\kappa_2 = \frac{\langle C_2 \rangle}{\langle\langle p_T \rangle\rangle^2}, \tag{23}$$

$$\kappa_3 = \frac{\langle C_3 \rangle}{\langle\langle p_T \rangle\rangle^3}, \tag{24}$$

$$\kappa_4 = \frac{\langle c_4 \rangle - 3\langle c_2 \rangle^2}{\langle\langle p_T \rangle\rangle^4} \tag{25}$$

where particles are taken from $|y_{CMS}|<1$ and only unique combinations of particles in the event are taken into account.

[Bhatta S. *et. al.* Phys. Rev. C 105, 024904]

Subevent method

$$\kappa_{2,sub} = \frac{\langle c_{2,2sub} \rangle}{\langle\langle p_T \rangle\rangle_f \langle\langle p_T \rangle\rangle_b} \tag{26}$$

$$\kappa_{3,2sub1} = \frac{\langle c_{3,2sub1} \rangle}{\langle\langle p_T \rangle\rangle_f^2 \langle\langle p_T \rangle\rangle_b}, \quad \kappa_{3,2sub2} = \frac{\langle c_{3,2sub2} \rangle}{\langle\langle p_T \rangle\rangle_f \langle\langle p_T \rangle\rangle_b^2} \tag{27}$$

$$\kappa_{4,2sub} = \frac{\langle c_{4,2sub} \rangle - 2\langle c_{2,2sub} \rangle^2 - \langle c_2 \rangle_a \langle c_2 \rangle_c}{\langle\langle p_T \rangle\rangle_a^2 \langle\langle p_T \rangle\rangle_c^2} \tag{28}$$

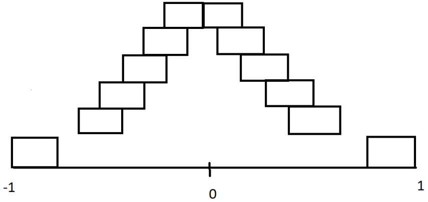

Figure 5: Intervals of rapidity that were chosen in the work for p+p collisions.

Results for strongly intensive variables: p+p

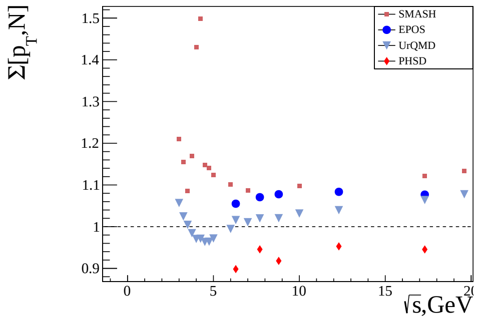

Figure 6: Dependence of $\Sigma[p_T, N]$ on beam energy for proton-proton collisions.

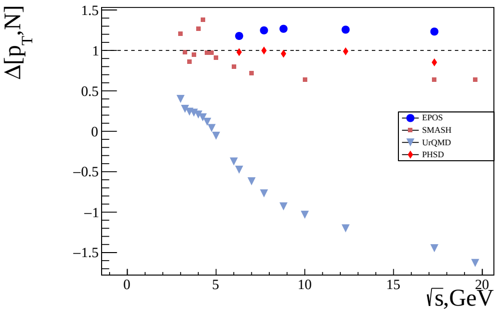

Figure 7: Dependence of $\Delta[p_T, N]$ on beam energy for proton-proton collisions.

- The transition from resonances to strings in the models generates a “wave”, which is observed on the graphs of $\Sigma[p_T, N]$ and $\Delta[p_T, N]$ for collision energy.
- Event selection criteria: $-1.0 < y_{CMS} < 1.0,\ 0.15 < p_T < 2.0\ GeV/c$.
- $\Delta[p_T, N] = \Sigma[p_T, N] = 1$ - value for the independent particle production model, $\Delta[p_T, N] = \Sigma[p_T, N] = 0$ - in the absence of fluctuations - deviation from these restrictions is observed

Results for highly intensive variables: p+p

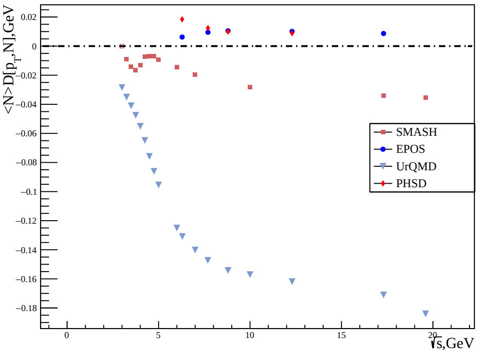

Figure 8: Dependence of $\langle N \rangle D[p_t, N]$ on beam energy.

$D \neq 0$ - PYTHIA/Angantyr [M. Cody, S. Gavin, B. Koch et al., Phys. Rev. C 107, 014909 (2023)].

Results for second and third order cumulants: p+p, UrQMD

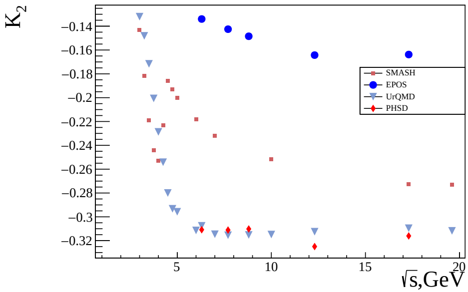

Figure 9: Dependence of the second-order cumulant for transverse momentum in proton-proton collisions.

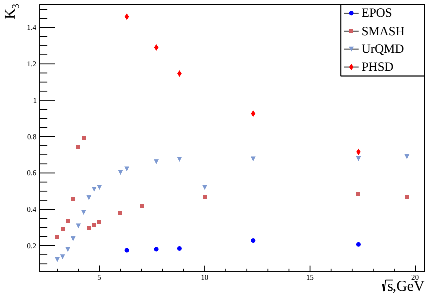

Figure 10: Dependence of the third order cumulant for transverse momentum in proton-proton collisions.

- HIJING - $\kappa_2 > 0$ $\kappa_3 > 0$. [S. Bhatta *et al.*, Phys. Rev. C 105, 024904].

Results of comparison of two methods for calculating cumulants: p+p, UrQMD

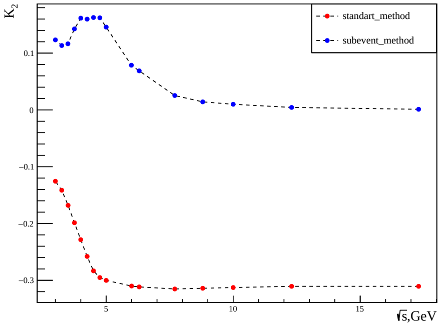

Figure 11: Dependence of the second-order cumulant for transverse momentum on energy in proton-proton collisions, calculated in two ways for the UrQMD model.

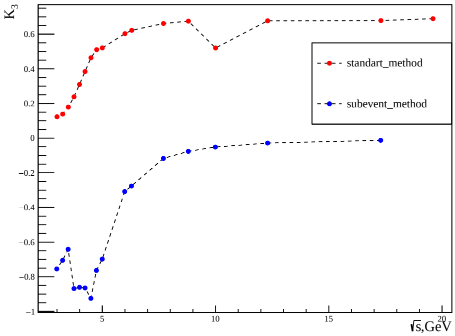

Figure 12: Dependence of the second-order cumulant for transverse momentum on energy in proton-proton collisions, calculated in two ways for the UrQMD model.

There is obvious discrepancy of the two methods.

Results of comparison of two methods for calculating cumulants: p+p, UrQMD

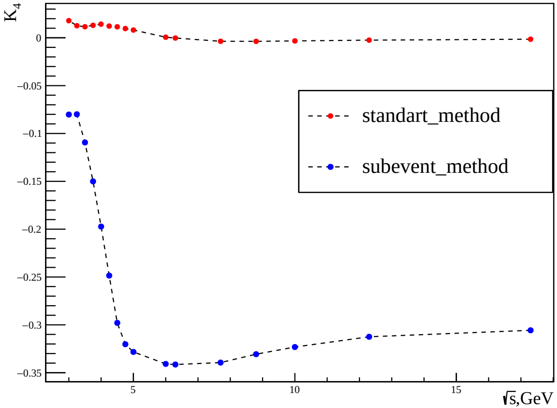

Figure 13: Dependence of the fourth-order cumulant for transverse momentum on energy in proton-proton collisions, calculated in two ways for the UrQMD model.

Results for subevent method for calculating cumulants: p+p, UrQMD

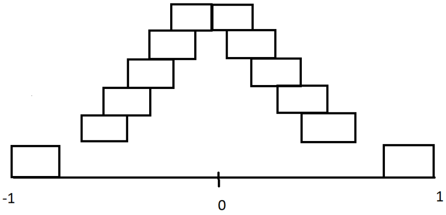

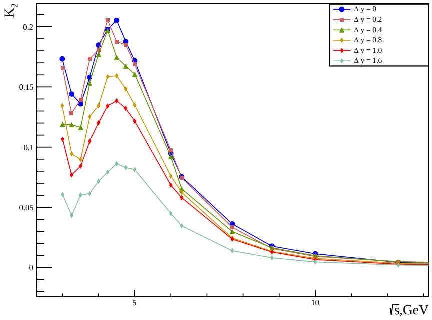

Figure 14: Dependence of the second order cumulant depending on the rapidity intervals.

There is a clear decrease in correlations with increasing distance between intervals of rapidity.

Results for second and third order cumulants: p+p

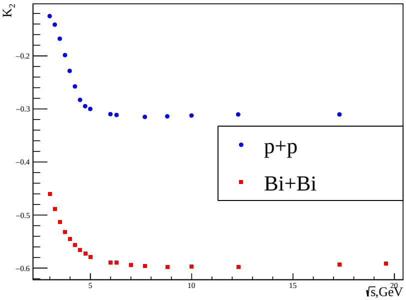

Figure 15: Dependence of the second-order cumulant for transverse momentum in proton-proton and Bi+Bi collisions.

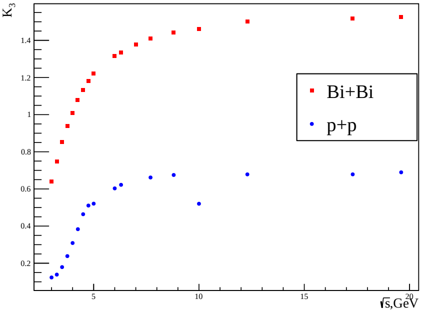

Figure 16: Dependence of the third order cumulant for transverse momentum in proton-proton and Bi+Bi collisions.

- HIJING - $\kappa_2 > 0$ $\kappa_3 > 0$. [S. Bhatta *et al.*, Phys. Rev. C 105, 024904].

Results for fourth order cumulants: Bi+Bi, UrQMD

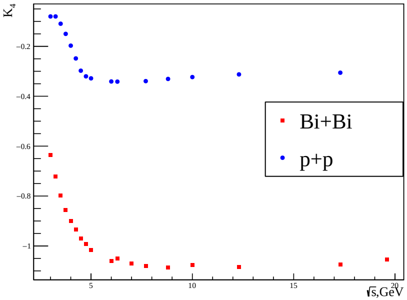

Figure 17: Dependence of the four-order cumulant for transverse momentum in proton-proton and Bi+Bi collisions.

- Dynamics of evolution and final-state interaction can lead to a deviation from this power-law behavior.
- Indeed, experimental measurements of p_T variance in $Au + Au$ collisions at $\sqrt{s_{NN}} = 200$ GeV and $Pb + Pb$ collisions at $\sqrt{s_{NN}} = 2.76$ TeV have reported the power to be ≈ 0.81 instead of the expected value of 1.
- This clear deviation from the baseline of independent source picture in the experimental data indicates the **presence of long-range collective correlations and significant final-state effects.**

Experimental results for cumulants from STAR: Au+Au, U+U

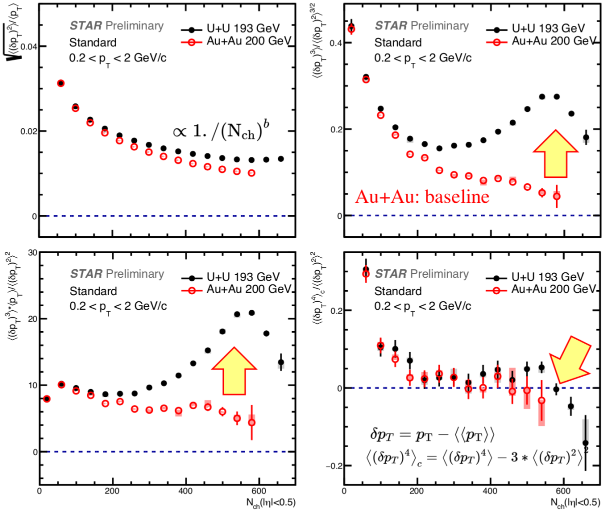

Figure 18: Experimental results from STAR collaboration [Chunjian Zhang, New results from flow, chirality and vorticity at RHIC-STAR].

Conclusions

• The SMASH model is an example of demonstrating the transition from the resonance regime to the string regime.
• A comparison is given of two different methods for calculating cumulants - the standard and the subevent method to eliminate short-range correlations. These methods give different results.
• Significant discrepancies are observed between the predictions of the EPOS, SMASH, PHSD, and UrQMD models, indicating that future data on $p+p$ collisions from the NICA experiment will constrain the predictions of these models and also refine results.
• The nontrivial dependence of p_T cumulants on collision energy predicted by models for the "basic" $p+p$ reaction highlights the difficulties in interpreting future results for $A+A$ collisions and requires further research
• The cumulants for the Bi+Bi reaction show approximately the same trend as the cumulants for $p+p$ collisions.
• This research supported by Saint Petersburg State University (ID: 94031112).

Back-up

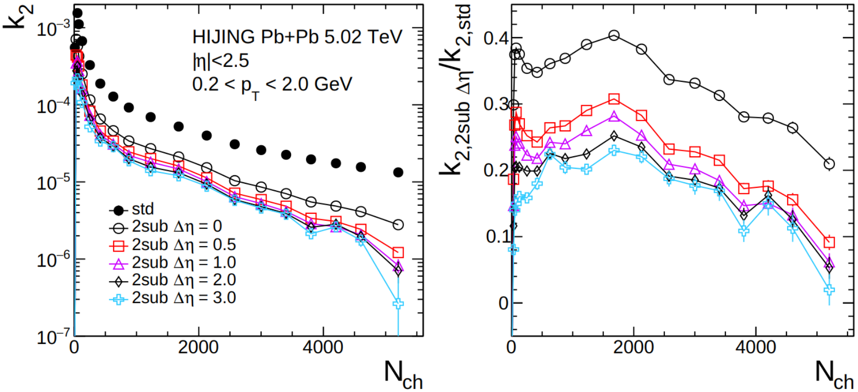

Figure 19: (Left) Variance obtained for the standard method and the subevent method with different rapidity intervals in $Pb + Pb$ collisions for $0.2 < p_T < 2$ GeV as a function of N_{ch}. (Right) Ratio of the results of the subevent method to the results of the standard method[S. Bhatta *et al.*, Phys. Rev. C 105, 024904].

Back-up

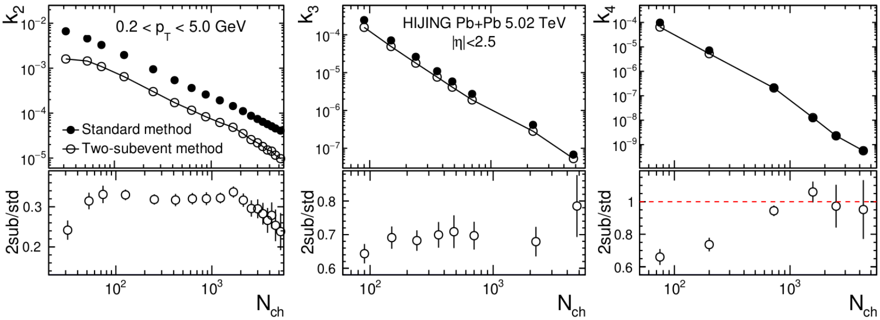

Figure 20: Second (left), third (center), and fourth (right) order moments in Pb+Pb collisions using standard (solid dots) and method of two subevents (empty dots) for charged particles in the range $0.2 < p_T < 5.0$ GeV depending on N_{ch}.[S. Bhatta *et al.*, Phys. Rev. C 105, 024904].

Back-up

In the subevent method (2subevent), combinations of particles are selected from two subevents separated by rapidity in CMS.

$a : (-0.2 < y_{CMS} < 0.0)$ $c : (0.0 < y_{CMS} < 0.2)$
$a : (-0.3 < y_{CMS} < -0.1)$ $c : (0.1 < y_{CMS} < 0.3)$
$a : (-0.4 < y_{CMS} < -0.2)$ $c : (0.2 < y_{CMS} < 0.4)$
$a : (-0.6 < y_{CMS} < -0.4)$ $c : (0.4 < y_{CMS} < 0.6)$
$a : (-0.7 < y_{CMS} < -0.5)$ $c : (0.5 < y_{CMS} < 0.7)$
$a : (-1.0 < y_{CMS} < -0.8)$ $c : (0.8 < y_{CMS} < 1.0)$

$$c_{2,2sub} = (\overline{p}_{11})_a (\overline{p}_{11})_c \tag{29}$$

$$c_{3,2sub1} = \frac{\left(\overline{p}_{11}^2 - \overline{p}_{22}\right)_a (\overline{p}_{11})_c}{1 - \tau_{1a}} \tag{30}$$

$$c_{3,2sub2} = \frac{\left(\overline{p}_{11}^2 - \overline{p}_{22}\right)_c (\overline{p}_{11})_a}{1 - \tau_{1c}} \tag{31}$$

$$c_4 = \frac{\left(\overline{p}_{11}^2 - \overline{p}_{22}\right)_a \left(\overline{p}_{11}^2 - \overline{p}_{22}\right)_c}{(1 - \tau_a)(1 - \tau_c)} \tag{32}$$

$2c_{3,2sub} = c_{3,2sub1} + c_{3,2sub2}$. [Bhatta S. *et. al.* Phys. Rev. C 105, 024904]

Back-up

$$p_{mk} = \sum_i \omega_i^k p_i^m / \sum_i \omega_i^k, \tau_k = \frac{\omega_i^{k+1}}{\left(\sum_i \omega_i\right)^{k+1}} \tag{33}$$

denoting $p \equiv p_T$:

$$\overline{p}_{1k} \equiv p_{1k} - \langle\langle p_T \rangle\rangle \tag{34}$$

$$\overline{p}_{2k} \equiv 2p_{1k}\langle\langle p_T \rangle\rangle + \langle\langle p_T \rangle\rangle^2 \tag{35}$$

$$\overline{p}_{3k} \equiv p_{3k} - 3p_{2k}\langle\langle p_T \rangle\rangle + 3p_{1k}\langle\langle p_T \rangle\rangle^2 - \langle\langle p_T \rangle\rangle^3 \tag{36}$$

$$\overline{p}_{4k} \equiv p_{4k} - 4p_{3k}\langle\langle p_T \rangle\rangle + 6p_{2k}\langle\langle p_T \rangle\rangle^2 - 4p_{1k}\langle\langle p_T \rangle\rangle^3 + \langle\langle p_T \rangle\rangle^4 \tag{37}$$

Note here

$$\langle\langle p_T \rangle\rangle = \langle p_{11} \rangle \tag{38}$$